An Automated Method for Rotational Correction and Centering of Three-Dimensional Functional Brain Images

Satoshi Minoshima, Kevin L. Berger, Kien S. Lee, and Mark A. Mintun

Division of Nuclear Medicine, Department of Internal Medicine, University of Michigan, Ann Arbor, Michigan

The display and analysis of functional brain images often benefit from head rotational correction and centering. An automated method was developed to align brain PET images into a standard three-dimensional orientation. The algorithm performs transverse and coronal rotational correction as well as centering of a brain image set. Optimal rotational correction and centering are determined by maximizing a bilateral hemispheric similarity index, the stochastic sign change criterion. Testing of this algorithm on simulated symmetrical brain image sets showed errors less than 1.0 degree and 0.5 pixels for rotational correction and centering, respectively. With actual PET data, the algorithm results correlated well with those obtained by visual inspection. Testing on asymmetrical brain image sets with simulated lesions indicated that performance of the algorithm is not sensitive to focal asymmetries. This automated method provides objective, reproducible image alignment into a standard orientation and facilitates subsequent data analysis techniques for functional brain images.

J Nucl Med 1992; 33:1579–1585

There are many situations in which correction of head rotation and right-left centering are essential for the analysis of functional brain images obtained by positron emission tomography (PET). Region of interest (ROI) analysis in brain studies, for example, is often based on a comparison between corresponding locations in the right and left hemispheres (*1–4*). This type of analysis cannot be achieved accurately without correction of head rotation and identification of the interhemispheric mid-sagittal plane of the brain. In addition, while several image alignment techniques have been described (*5–7*), these only work in two dimensions (intraslice) and require correction of the head tilt (coronal rotation) prior to their application.

Techniques using a head holder to allow direct correlation of PET data to an anatomical coordinate space (e.g., with a magnetic resonance image) may avoid image manipulations such as rotational correction and interslice interpolation (*8–12*). However, reslicing and reformatting of PET images after data acquisition become more acceptable with increasing intraslice and interslice sampling (*13*). Even with a headholder to fix the head in a certain position, some movement cannot be completely eliminated (*6,8*), and the retrospective correction of head rotation may prove helpful.

Alternatively, anatomical localization can be based on the direct fitting of the intercommissural (the anterior commissure-posterior commissure or AC-PC) line using only PET images (*14,15*). In this case, the mid-sagittal slice of PET images typically must be determined for the direct fitting of the line, a procedure which involves correction of head rotation and right-left centering of the images.

A method for transverse rotational correction and right-left centering has been described by Junck et al. (*7*). In this approach, the right and left hemispheres are assumed to be symmetrical, and a part of the numerator of the correlation coefficient, calculated from corresponding pixel values across the midline, is used as an index of image alignment. This method appeared to work better than visual inspection in normal PET images. However, the assumption requiring right-left brain symmetry limits this method since brain symmetry cannot be presupposed in many pathological cases. Also, this method did not correct head rotation in the coronal plane. To address these problems, we have developed a new automated technique for simultaneous correction of transverse and coronal head rotation and right-left centering using the stochastic sign change (SSC) criterion as an index of image alignment.

The SSC criterion was first described by Venot et al. (*16–18*) for the normalization and registration of planar scintigraphic images. Mintun and Lee expanded this concept to the three-dimensional registration of PET images, enabling registration between sets of PET images from the same subject obtained on different days (*19*). The SSC criterion originally was derived from the summation of all the sign changes in the image created by subtracting one of the original images from the other image. When applied

Received Dec. 24, 1991; revision accepted Mar. 27, 1992.

For reprints contact: Mark A. Mintun, MD, Division of Nuclear Medicine, Department of Radiology, Univeristy of Pittsburgh, Presbyterian University Hospital, DeSoto at O'Hara Streets, Pittsburgh, PA 15213.

to the registration of two similar but nonidentical images from the same subject, the SSC criterion was demonstrated to be far more robust for registration of the images than other methods, including those based on the correlation coefficient (*17*). In this paper, we describe the application of the SSC criterion to transverse and coronal rotational correction and right-left centering, and we validate this method using normal brain PET image sets, simulated symmetrical brain image sets, and simulated asymmetrical brain image sets containing various types of focal lesions.

THEORETICAL METHODS

Rotational Correction and Centering in Three Dimensions

Rotational correction and centering assume a gross symmetry of the right and left hemispheres of the brain. The mid-sagittal plane is determined iteratively by optimizing similarity of the right and left hemispheric activity distributions in a given PET image set since maximal right-left similarity should be obtained about the mid-sagittal plane of the brain (*7*). The similarity between the right and left hemispheric activities actually is calculated using a given PET image set and its "mirror" image set created by flipping the given image set about a presumed mid-sagittal plane.

In the algorithm, let the spatial coordinates X, Y, Z be the right-left, anterior-posterior, top-bottom axes, respectively, of the head in a PET image set. The search routine starts from rotation of a PET image set around the center of the image matrix by given angles Δqz and Δqy in transverse (XY) and coronal (XZ) planes respectively to create a rotated original image set $I_{org}(x,y,z)$. Then the $I_{org}(x,y,z)$ is flipped about a presumed mid-sagittal plane at a given X position (Δx) to create the flipped rotated image set $I_{flip}(x,y,z) = I_{org}(2 \cdot \Delta x\text{-}x,y,z)$. The similarity index SSCxyz is calculated between the $I_{org}(x,y,z)$ and the $I_{flip}(x,y,z)$ by the stochastic sign change criterion adapted for three-dimensional image sets. Consequently, the index SSCxyz is expressed as a function of Δqz, Δqy and Δx. These steps are repeated by a multidimensional search routine until the maximum SSCxyz is detected, where the right and left hemispheric activity distributions are most complementary (see Appendix). The Δqz, Δqy and Δx at the maximum SSCxyz indicate the location of the mid-sagittal plane in the PET image set. Once the mid-sagittal plane is determined, the brain image set can be transformed in a standard orientation, matching the mid-sagittal plane to the center plane of the image matrix.

Application of the SSC Criterion for Three-Dimensional Rotational Correction and Centering

The stochastic sign changed criterion as a similarity index originally has been described for two-dimensional image registration (*16–18*) (see Appendix). Briefly, the SSC can be used to co-register two images that contain a significant amount of random noise. If the two images are well co-registered, the maximum random fluctuation of pixel values and zero-crossing points (sign changes) are observed in a subtraction image between those two images.

In the situation of rotational correction and centering, the two images to be registered using SSC are the PET image set $I_{org}(x,y,z)$ and its flipped image set $I_{flip}(x,y,z)$ previously described. In the subtraction image set $I_{org}(x,y,z) - I_{flip}(x,y,z)$, all sign changes are summed first along the x-axis in each line, from anterior to posterior in each transverse slice (*17,18*) and from the top slice to the bottom slice. Summation of all SSC values obtained from each slice is defined as SSCx. Then, SSCy is calculated along the y-axis in a line, from top to bottom in each sagittal slice and from the right to the left sagittal slices. SSCz is calculated along the z-axis in a line, from right to left in each coronal slice and from the anterior to the posterior coronal slices. SSCxyz is defined as the summation of SSCx, SSCy, and SSCz and consequently represents the image similarity in all three directions.

When applying the SSCxyz, small but systematic differences between overall right and left hemispheric activities could cause greatly decreased sign changes in the subtraction image $I_{org}(x,y,z) - I_{flip}(x,y,z)$, even if anatomical structures of the right and left hemispheres are perfectly symmetrical. This would decrease the accuracy of the algorithm. To avoid this problem, a periodic pattern is added on the $I_{org}(x,y,z)$ in the following manner:

$$I_{org'}(x,y,z) = I_{org}(x,y,z) \times (1.0 + p) \text{ if } x+y+z \text{ is even,}$$

$$I_{org'}(x,y,z) = I_{org}(x,y,z) \times (1.0 - p) \text{ if } x+y+z \text{ is odd,}$$

where p is a small fraction ($p = 0.0625$ in this study, see Discussion). By adding the p value, a significant number of sign changes could still be generated in the subtraction image even if pixel values of corresponding areas in the right and left hemispheres differ on average by up to ($p \times 100$)%. The SSCxyz is thus obtained from a subtraction image $I_{org'}(x,y,z) - I_{flip}(x,y,z)$ instead of $I_{org}(x,y,z) - I_{flip}(x,y,z)$.

MATERIALS AND METHODS

PET Scans

Fluorine-18-2-fluoro-2-deoxy-D-glucose (FDG) PET image sets were collected from twenty normal subjects to validate the method. Each study was performed using either one of two identical Siemens 931/08-12 whole-body scanners (CTI Inc., Knoxville, TN) in our laboratory, which collects 15 simultaneous slices with a slice-to-slice separation of 6.75 mm (*20*). Each subject was carefully positioned in the tomograph using laser beam guides in planes of the canthomeatal line and cranial midline. Two sequential interlaced (by 1/2 slice) emission scans of 30 min each were taken beginning 30 min after intravenous injection of 10 mCi (370 MBq) of FDG. The scans were attenuation corrected with two 10-min interlaced transmission scans and reconstructed with a Shepp filter cutoff frequency of 0.35 cycles per pixel, giving an in-plane FWHM of approximately 7

mm. The reconstructed image matrix had 128 × 128 pixels with 1.875 mm size. While two emission scans were collected, only the latter image set of 15 slices beginning 1 hr after FDG injection was used in this study.

Implementation of the Algorithm

The automated program, which includes the rotational correction and centering as well as pre-processing of the original PET image set (see Appendix), was written in C language and implemented on the SUN SPARC station (Sun Microsystems, Mountain View, CA). The program generates a transformation parameter file containing optimal Δqz, Δqy and Δx values, as well as realigned image set. The parameter file indicates rotation and translation of the brain and can be used by other image processing routines.

Validation: Basic Performance of the Algorithm

Accuracy of this algorithm was tested using five simulated symmetrical image sets. Each simulated symmetrical image set was created from a different normal FDG PET study in the following way. First, using a user-interactive image processing program, transverse and coronal rotation of the brain in an original PET image set was examined by visual inspection. After the rotation of the brain was corrected, the mid-sagittal plane was determined visually. The image set was translated to match the mid-sagittal plane with the center of the image matrix. Then, the left hemisphere was entirely removed from the image set, and the right hemisphere was flipped about the mid-sagittal line and copied onto the space where the left hemisphere had existed. As a result, the simulated image set was symmetrical about the mid-sagittal line at the center of the image matrix (Fig. 1). To change the statistical noise in each hemisphere, small random uniform noise between −0.1% to 0.1% of the original pixel value was added to each pixel. Without this procedure, no sign changes instead of the maximum number of sign changes essentially will be observed when the simulated symmetrical image set is perfectly aligned in a symmetrical position.

To test the accuracy of the algorithm, all five simulated image sets were rotated around the center of the image matrix in the transverse and coronal planes using different combinations of angles chosen from 0, 1, 2, 4, 8 or 16° for transverse rotation and from 0, 1, 2, 4 or 8° for coronal rotation. Thirty combinations of rotational angles for five image sets created 150 rotated image sets. All rotated image sets were translated five pixels in the X direction to test the centering accuracy. The rotated and translated image sets were reformatted to match the pixel size, slice separation, and number of slices of the original PET studies. Subsequently, all image sets were processed by the automated program to calculate rotational angles (transverse and coronal) and translation (centering). Accuracy of the rotational correction was calculated from the difference between preset rotational angles and angles determined by the program for both transverse and coronal directions. Also, accuracy of the centering was calculated from the difference between the pretranslated center and the mid-sagittal line of the brain determined by the program.

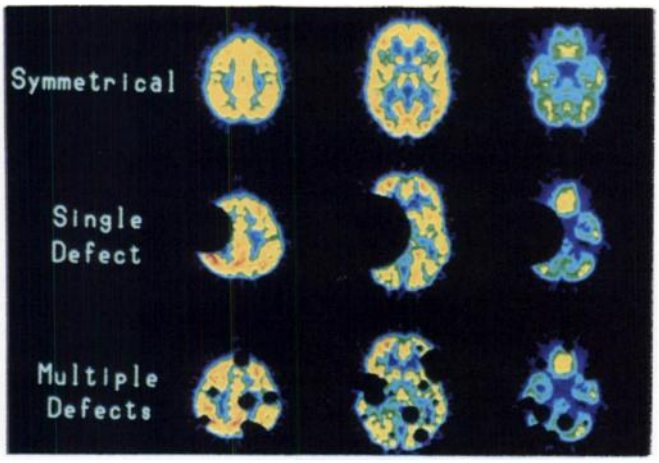

FIGURE 1. Examples of a simulated symmetrical brain image set and asymmetrical brain images with single and multiple lesions. These images were used in validations.

Comparison with Visual Inspection

Rotation and centering of the brain were also examined in 20 normal FDG PET studies by the automated program. These results were compared with visual inspection of rotation and centering. With use of an interactive image processing program, two investigators independently examined the rotation and centering of the studies. The transverse rotation was first determined using the original fifteen transverse slices, and then the coronal rotation was determined from the reformatted fifteen coronal slices after transverse rotational correction. Centering was performed after the transverse and coronal rotational correction. The minimum steps in the interactive program were 0.1° for the rotations and 0.25 pixels for the translation. When examined visually, the investigators considered anatomical landmarks, including cerebral falx, anterior and posterior cingulate gyri, heads of caudate nuclei and bilateral thalamus, to decide the mid-sagittal plane of the brain while the cerebral cortex, which appeared to have some normal right-left asymmetry in many subjects, was not heavily weighted in deciding the mid-sagittal plane. Results from two visual inspections were averaged, and differences between computed and visual values were summarized for transverse and coronal rotation and centering. Also, the accuracy of initial positioning of the head with laser beam guidance in these 20 subjects was assessed by comparison with the amount of correction measured by the automated program. A two-tailed paired t-test was applied for statistical analysis.

Application to Asymmetrical Brains

A lack of symmetry between the cerebral hemispheres could impede the detection of the mid-sagittal plane as well as the correction of head rotation. The algorithm was validated to be applicable in asymmetrical brains with single or multiple lesions. In simulations with a single lesion, a lesion of 1%, 2%, 4%, 8%, 16% or 32% of the total brain volume was placed in the temporoparietal lobe of a PET image set (Fig. 2A). The brain volume was calculated by counting the number of voxels within the brain in the field of view of PET imaging. The shape of the lesion was basically spherical unless the lesion was abutting the brain edge. Five normal FDG studies were modified with each size lesion, creating thirty image sets. In simulations with multiple lesions, 1, 2, 4, 8, 16 or 32 lesions (each lesion having 1% volume of the brain) were placed randomly in a PET image set using a random number generator (Fig. 2B). The center of each lesion was located in gray matter, defined as voxels more than 50% of the peak voxel value. Five normal FDG studies were modified with each number of lesions, creating thirty image sets. In simulations of either single or multiple lesions, reduced activities of either 50% or 100% of the original voxel value in the lesion were assumed,

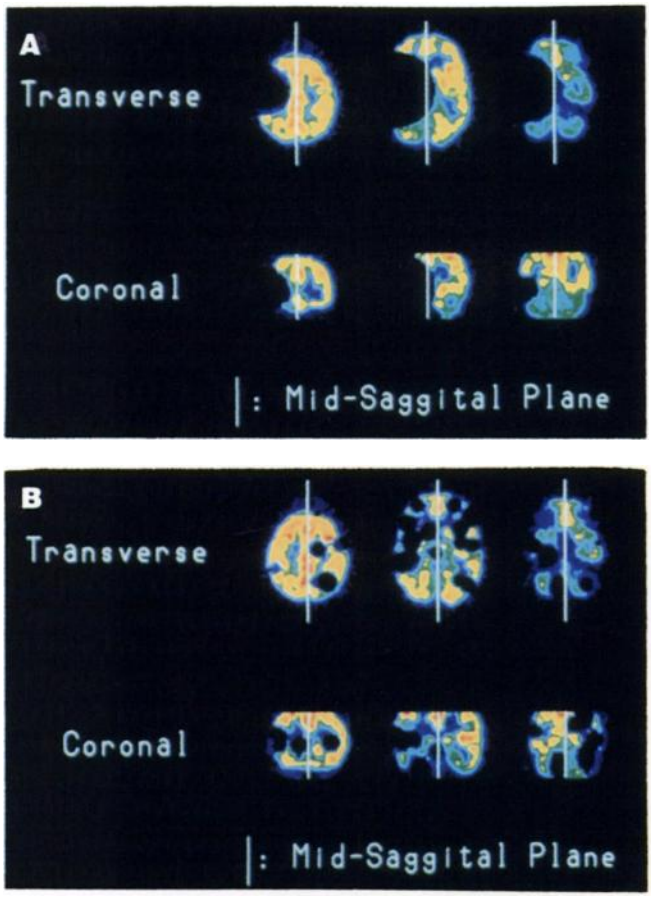

FIGURE 2. (A) Example of a brain FDG PET image set with a single simulated lesion. The lesion occupies 32% of the brain volume with 100% reduction of original activity. A white line in the image indicates the center line of the brain determined by the algorithm after transverse and coronal rotational correction. In spite of the large lesion, the algorithm can correct head rotation and finds the mid-sagittal line of the brain with minimal error. (B) Example of brain FDG PET image set with multiple simulated lesions. Thirty-two lesions are put in the brain at random. Each lesion occupies 1% by volume of the brain with 100% reduction of original activity. A white line indicates the mid-sagittal line of the brain determined by the algorithm. The algorithm works well with multiple as well as single lesions.

generating a total of 120 modified asymmetrical image sets (60 with a single lesion, 60 with multiple lesions). The simulated image sets were reformatted to match the pixel size, slice separation and number of slices of the original PET studies. The automated program was applied to all of these asymmetrical image sets, and the results were compared with values obtained from the original normal image sets without the simulated lesions. In each image set, the error was defined by the absolute value of the difference obtained from the original image set and the simulated-lesion image set. Errors were summarized for the transverse and coronal rotational correction and the centering for each combination of lesion volume and reduced activity.

RESULTS

Basic Performance of the Algorithm

From a total of 150 simulated symmetrical image sets rotated by various combinations of angles, the algorithm determined the rotational correction and centering precisely. For the transverse rotational correction, the overall averaged error was 0.03°, and the maximum error was 0.2°. Most of the transverse rotations were corrected exactly. For the coronal rotational correction, the overall averaged error was 0.1°, and the maximum error was only 0.3°. For the centering, errors were always within one step (0.5 pixels) of the X translation routine. The rotational corrections and centering were performed consistently and accurately within the given combinations of preset rotational angles.

Comparison with Visual Inspection

Computed values of the rotation and centering were compared with visual inspection in twenty brain PET studies from normal subjects. Mean differences between computed values and visual values were small: 0.4 ± 0.3° (mean ± s.d.) in the transverse rotation, 0.5 ± 0.2° in the coronal rotation and 0.2 ± 0.2 pixels in the centering. The largest discrepancies were 0.9° in the transverse rotation, 0.9° in the coronal rotation and 0.4 pixels in the centering. No statistically significant differences ($p > 0.05$) were observed between computed and visual values in the transverse and coronal rotation and centering.

For the 20 normal scans in which subjects' heads were positioned using the laser beam guide, the program detected a mean value of 1.2 ± 0.9° for transverse rotation, 1.2 ± 0.7° for coronal rotation and 1.4 ± 1.2 pixels for the displacement between the mid-sagittal line of the brain and center of the image matrix.

Application to Asymmetrical Brains

The algorithm also worked well with the one-hundred twenty asymmetrical image sets containing various lesions. For image sets with a single lesion (Table 1, Fig. 2A), most rotational correctional errors were within one step of the search routines (0.2°). The errors tended to increase with larger lesion volumes, and the maximum rotational correctional errors were observed in coronal rotation with image sets containing a single lesion of 32% volume of the brain. Even in such cases, errors in coronal rotation were within 1.0°. There was no centering error for most image sets. For image sets with multiple defects (Table 2, Fig. 2B), most rotational correctional errors were within three steps (0.6°). The largest error was 0.8° in coronal rotation with the image set containing 32 defect lesions of 50% reduced activity. Centering was also accurate with no error observed in the image sets with multiple defects. Asymmetry of the brain as a result of various lesions had a surprisingly minimal effect on the rotational correction and centering performance of the algorithm.

DISCUSSION

The algorithm presented here works accurately and consistently with not only symmetrical image sets but also asymmetrical image sets. For both transverse and coronal rotational corrections, errors in simulated symmetrical

TABLE 1
Errors Caused by Various Single Lesions in Simulated Asymmetrical Brain Images

Reduction of activity in a simulated lesion	Errors	Size of a simulated single lesion (%volume of the whole brain)					
		0.0	2.0	4.0	8.0	16.0	32.0
50%	Transverse*	0.1 ± 0.1	0.1 ± 0.1	0.1 ± 0.2	0.1 ± 0.2	0.5 ± 0.6	0.3 ± 0.4
	Coronal†	0.1 ± 0.2	0.2 ± 0.2	0.2 ± 0.1	0.2 ± 0.1	0.2 ± 0.1	1.0 ± 0.9
	Centering‡	0.0 ± 0.0	0.0 ± 0.0	0.0 ± 0.0	0.0 ± 0.0	0.1 ± 0.2	0.1 ± 0.2
100%	Transverse*	0.1 ± 0.1	0.2 ± 0.2	0.1 ± 0.2	0.1 ± 0.2	0.4 ± 0.5	0.3 ± 0.4
	Coronal†	0.2 ± 0.2	0.3 ± 0.1	0.2 ± 0.1	0.2 ± 0.1	0.2 ± 0.1	1.0 ± 0.7
	Centering‡	0.0 ± 0.0	0.0 ± 0.0	0.0 ± 0.0	0.0 ± 0.0	0.1 ± 0.2	0.1 ± 0.2

Mean ± s.d. (n = 5).
* Errors of transverse rotational correction (degrees).
† Errors of coronal rotational correction (degrees).
‡ Errors of centering (pixels).

image sets were within 0.28°. Assuming the furthest edge of a brain from a center is 10 cm, the maximum error of rotational correction will cause a translational error of only 0.5 mm at the edge. The accuracy of the algorithm allowed for almost no error in centering in this series of validations. Since the step size of centering was 0.5 pixels (1.125 mm), centering errors were within a maximum of 0.56 mm. The automated method achieved a high degree of accuracy completely objectively.

In 20 normal subjects, computed values for rotational correction and centering agreed well with averaged values of independent visual inspections. The mean difference between computed and visual results in transverse rotational correction was 0.37 ± 0.28° (n = 20); this mean value was approximately equal to the mean value 0.54 ± 1.16° (n = 37) obtained by the correlation method (*7*). However, the variance was significantly smaller than that by the correlation method (two-tailed variance ratio test, $p < 0.01$). To examine this effect more closely, we replaced the SSC criterion with the correlation method in our algorithm and applied this routine to just transverse rotational correction in 20 normal FDG scans. This data showed that discrepancies with visual inspection were 0.44 ± 0.38° by the SSC criterion versus 0.61 ± 0.77° by the correlation method. According to the simulation study reported by Venot et al. (*17*), the SSC, as an index of similarity measurement, was more robust and consistent than the correlation coefficient when two images were dissimilar. Junck et al. (*7*) also mentions the limitation of the correlation method in asymmetrical brains due to focal lesions.

The accuracy of the SSC algorithm, however, was unaffected by focal asymmetries in the brain. In the most extreme example, a brain containing a large lesion occupying 32% of the volume of the brain with 100% reduction of activity produced only a 1.0° error in rotational correction and 0.1 pixel error in centering. We also would expect the algorithm should perform equally well with image sets containing "hot spots" because those areas would result in the same type of sign changes as "cold" lesions. Since the algorithm still requires a certain degree of symmetry between right and left hemispheres for rotational correction and centering, errors will likely be found in studies with severe global asymmetry. This situation may occur in patients with substantial hemispheric removal, severe asymmetrical atrophy, massive necrosis after irradiation, etc.

When adapting the SSC criterion to rotational correc-

TABLE 2
Errors Caused by Various Multiple Lesions in Simulated Asymmetrical Brain Images

Reduction of activity in simulated lesions	Errors	Number of simulated multiple lesions					
		0	2	4	8	16	32
50%	Transverse*	0.2 ± 0.2	0.2 ± 0.1	0.2 ± 0.3	0.2 ± 0.2	0.2 ± 0.2	0.4 ± 0.4
	Coronal†	0.3 ± 0.4	0.4 ± 0.4	0.3 ± 0.4	0.5 ± 0.4	0.6 ± 0.5	0.6 ± 0.4
	Centering‡	0.0 ± 0.0	0.0 ± 0.0	0.0 ± 0.0	0.0 ± 0.0	0.0 ± 0.0	0.0 ± 0.0
100%	Transverse*	0.2 ± 0.2	0.2 ± 0.2	0.2 ± 0.4	0.1 ± 0.2	0.2 ± 0.3	0.4 ± 0.4
	Coronal†	0.2 ± 0.1	0.5 ± 0.4	0.3 ± 0.4	0.5 ± 0.4	0.5 ± 0.3	0.8 ± 0.5
	Centering‡	0.0 ± 0.0	0.0 ± 0.0	0.0 ± 0.0	0.0 ± 0.0	0.0 ± 0.0	0.0 ± 0.0

Mean ± s.d. (n = 5).
* Errors of transverse rotational correction (degrees).
† Errors of coronal rotational correction (degrees).
‡ Errors of centering (pixels).

tion and centering, one problem arose from slight or moderate global asymmetry of the right and left hemispheric activities. A small, but significant, difference in glucose utilization between the right and left hemispheres in normal subjects, for example, has been reported using FDG PET (*4*). In this situation, SSC values calculated between the right hemisphere and the flipped left hemisphere would decrease, and the SSC values could become influenced only by a small parts of the right and left hemispheres where equal activities were still present. To avoid this problem, a periodic p value was added onto the image set when calculating the sign changes. The relationship between p values and its effect on accuracy of rotational correction and centering was examined prior to this study (Fig. 3). With small p values under 0.05, the SSC values were smaller and the discrepancies between visual inspection and computed correction were larger. With increasing p values, the SSC values increased, and the discrepancies became smaller and kept steady with p values of 0.05 to 0.20. The p value can be minimized if greater symmetry of the right and left activities of the brain can be assumed. Although the p value should be increased as the hemispheric activities become more asymmetrical, the larger p values lose fine contrast of the activity distribution in the brain and may cause significant errors. In the current program in our laboratory, p = 0.0625 is used and excellent results have been obtained for FDG and ^{15}O water PET image sets. This modification looks similar to the deterministic sign change (DSC) criterion also described by Venot et al. (*17*); however, the values added to the image set as the periodic pattern are larger than those in the DSC and serve a different purpose. Small periodic values were added in the DSC when noise level in corresponding areas of images was too low to create a significant number of sign changes, while the p values were added in this algorithm to allow sign changes in corresponding areas of right and left hemispheres where measured activities were slightly different. Of course, if the noise level in a PET image set is significantly low from the use of a reconstruction filter with a low cutoff frequency and/or filtering, the periodic p value will create a DSC-like effect and will compensate for the otherwise small number of sign changes.

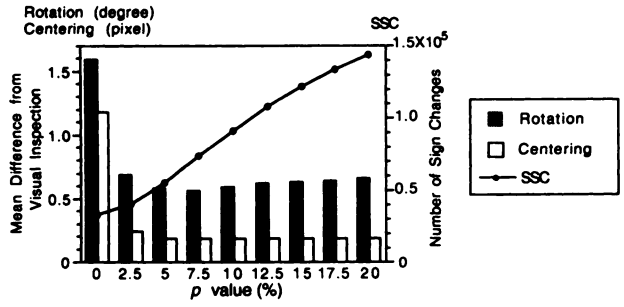

FIGURE 3. Relationship between p value and performance of the algorithm. Rotational correction and centering were examined with various p values in five normal images and five asymmetrial images containing a single lesion of 32% by volume of the brain with 100% reduction of activity. Mean differences between values calculated by the algorithm and values obtained by visual inspection were averaged over ten images in each p value. Errors in transverse and coronal rotational corrections were averaged. The maximum number of sign changes calculated by the algorithm in each image was also averaged. The number of sign changes increased with larger p values, and the mean differences were minimized with p values greater than 5%. In the algorithm, 6.25% was used.

In the data acquired for this study, a subject's head was carefully positioned into the PET gantry using laser beam guides in the plane of the canthomeatal line and the cranial midline. The algorithm detected correctable rotations that averaged 1.2° for transverse and coronal planes. Since significant differences of glucose metabolic rate in ROI analysis with only one pixel shift (2.8 mm) have been reported (*6*), correction of such a small misalignment may be indispensable for various kinds of data analysis and precise localization of PET studies. Although considerable accuracy in PET image alignment may be obtained by using a headholder or mask (*8–12*), a few degrees or millimeters of misalignment should not be neglected (*6,8*), and correction by the algorithm would still be applicable. Image alignment after scanning is now particularly useful with increasing sampling and spatial resolution of PET, which greatly decrease reslicing errors and related partial volume effects (*13*).

The procedures of transverse and coronal rotational correction and centering are equivalent to detection of the mid-sagittal plane in PET studies. Localization of PET images using direct fitting of the AC-PC line has been previously reported (*14*), where the mid-sagittal plane must be determined prior to the line fitting. Furthermore, in combination with an automated detection method of the AC-PC line (*15*), the algorithm would allow fully automated registration of PET image sets into a stereotactic coordinate system. Although normal variations or pathological distortion of brain structures in the stereotactic coordinate system should be considered (*14,21*), this combination provides a retrospective localization method of PET images without additional anatomical imaging by MRI or CT (*5,9,11,22–25*). Implementation to data processing systems can be fully automated without the requirement of visual inspection and image manipulation by experts (*6,25,26*). Also, the algorithm could be easily adapted to brain studies obtained by SPECT. A computation time for one image set takes approximately 20 min using a common commercial workstation. This short execution time makes the automated method practical in both clinical and research situations. Batch processing becomes possible with the automated method and is suitable for retrospectively dealing with a large number of subjects as well as for routine use.

The application of the SCC criterion (*16–18*) provides

an accurate, robust method for rotational correction and centering of symmetrical and asymmetrical brains, and it may facilitate subsequent data analysis techniques for brain PET images.

APPENDIX

The SSC Criterion

Consider two similar but not identical images $I_1(x,y)$ and $I_2(x,y)$ from the same region in the same subject, where $I(x,y)$ is the pixel count and $x,y = 1.2, \ldots n$ are the coordinates of the digitized images. Let $S(x,y) = I_1(x,y) - I_2(x,y)$ be the subtraction image. If $I_1(x,y)$ and $I_2(x,y)$ contain additive noise which can be assumed to have a zero mean with a symmetric density function, each pixel value of $S(x,y)$ is not zero but shows random fluctuations around zero, either positive or negative values with equal probability. If there is a dissimilar part of the images between $I_1(x,y)$ and $I_2(x,y)$, the pixel values of $S(x,y)$ in that part will no longer exhibit random fluctuations and will show groupings of all positive or negative values. Let SSC represent the number of sign changes in a sequence of the $S(x,y)$, scanned line-by-line or column-by-column. Accordingly, SSC shows a larger number of sign changes when $I_1(x,y)$ and $I_2(x,y)$ are similar and a lower value when $I_1(x,y)$ and $I_2(x,y)$ are dissimilar. Therefore, the SSC criterion can be defined as a similarity criterion between two images.

Optimization of the Similarity Index

To maximize the SSCxyz, a simple grid search was used in the program: First, a global search was conducted within present domains ($-16.0 \leq \Delta qz \leq +16.0°$ and $-16.0 \leq \Delta qy \leq +16.0°$ with 1.0° step, $-10 \leq \Delta x \leq +10$ pixels with 0.5 pixel step), then followed by a fine adjustment about the value with the highest SSCxyz using 0.2° step for Δqz and Δqy and 0.5 pixels step for Δx. As long as a subject's head is positioned into a PET gantry by a laser guide, these preset domains are sufficient.

Preprocessing of a PET Image Set

At the beginning of the automated program, the original PET image set of 15 slices was resampled by a three-dimensional linear interpolation to create an image set of 128 × 128 matrix size and 43 slices with uniform 2.25 mm voxel size. Subsequent image manipulations were done in this matrix space. The top six and bottom nine slices were then discarded (set to zero) because they often contained many nonbrain voxels. Voxels with less than 40% of the average voxel value of the brain were considered outside the brain and set to zero. The average voxel value of the brain was determined using all voxels more than 25% of the peak voxel value. Since, these cutoff thresholds were determined empirically from FDG and ^{15}O-water studies, some adjustment could be required for other types of functional images.

ACKNOWLEDGMENTS

The authors thank Robert A. Koeppe, Gary D. Hutchins for helpful advice, Jill Rothely, CNMT and other technologists of the PET suite for skillful performance of the studies. Dr. Mintun was supported as a Research and Education Foundation Scholar of the Radiological Society of North America. Kevin L. Berger was supported by a Student Fellowship Award from the Education and Research Foundation of the Society of the Nuclear Medicine.

REFERENCES

1. Duara R, Grady G, Haxby J, et al. Human brain glucose utilization and cognitive function in relation to age. *Ann Neurol* 1984;16:702–713.
2. Horowitz B, Duara R, Rapoport SI. Intercorrelations of glucose metabolic rates between brain regions: application to healthy males in a state of reduced sensory input. *J Cereb Blood Flow Metab* 1984;4:484–499.
3. Junck L, Gilman S, Rothley JR, Betley A, Koeppe RA, Hichwa RD. A relationship between metabolism in frontal lobes and cerebellum in normal subjects studied with PET. *J Cereb Blood Flow Metab* 1988;8:774–782.
4. Tyler JL, Strother SC, Zatorre RJ, et al. Stability of regional cerebral glucose metabolism in the normal brain measured by positron emission tomography. *J Nucl Med* 1988;29:631–642.
5. Alpert NM, Bradshaw JF, Kennedy D, Correia JA. The principal axes transformation—a method for image registration. *J Nucl Med* 1990;31: 1717–1722.
6. Phillips RL, London ED, Links JM, Cascella NG. Program for PET image alignment: effects on calculated differences in cerebral metabolic rates for glucose. *J Nucl Med* 1990;31:2052–2057.
7. Junck L, Moen JG, Hutchins GD, Brown MB, Kuhl DE. Correlation methods for centering, rotation, and alignment of functional brain images. *J Nucl Med* 1990;31:1220–1276.
8. Seitz RJ, Bohm C, Greitz T, et al. Accuracy and precision of the computerized brain atlas programme for localization and quantification in positron emission tomography. *J Cereb Blood Flow Metab* 1990;10:443–357.
9. Evans AC, Beil C, Marrett S, Thompson CJ, Hakim A. Anatomical-functional correlation using an adjustable MRI-based region of interest atlas with positron emission tomography. *J Cereb Blood Flow Metab* 1988;8:513–530.
10. Zhang J, Levesque MF, Wilson CL, et al. Multimodality imaging of brain structures for stereotactic surgery. *Radiology* 1990;175:435–441.
11. Meltzer CC, Bryan RN, Holcomb HH, et al. Anatomical localization for PET using MR imaging. *J Comput Assist Tomogr* 1990;14:418–426.
12. Fox PT, Perlmutter JS, Raichle ME. A stereotactic method of anatomical localization for positron emission tomography. *J Comput Assist Tomogr* 1985;9:141–153.
13. Correia JA. Registration of nuclear medicine images. *J Nucl Med* 1990;31:1227–1229.
14. Friston KJ, Passingham RE, Nutt JG, Heather JD, Sawle GV, Frackowiak RSJ. Localisation in PET images: direct fitting of the intercommissural (AC-PC) line. *J Cereb Blood Flow Metab* 1989;9:690–695.
15. Minoshima S, Berger KL, Lee KS, Taylor SF, Mintun MA. Automated detection of the intercommissural (AC-PC) line for stereotactic registration of PET images [Abstract]. *J Nucl Med* 1991;32:966.
16. Venot A, Lebruchec JF, Golmard JL, Roucayrol JC. An automated method for the normalization of scintigraphic images. *J Nucl Med* 1983;24:529–531.
17. Venot A, Lebruchec JF, Roucayrol JC. A new class of similarity measures for robust image registration. *Comput Vis Graph Image Process* 1984;28:176–184.
18. Venot A, Liehn JC, Lebruchec JF, Roucayrol JC. Automated comparison of scintigraphic images. *J Nucl Med* 1986;27:1337–1342.
19. Mintun MA, Lee KS. Mathematical realignment of paired PET images to enable pixel-by-pixel subtraction [Abstract]. *J Nucl Med* 1990;31:816.
20. Spinks TJ, Jones T, Gilardi MC, Heather JD. Physical performance of the latest generation of commercial positron scanner. *IEEE Trans Nucl Sci* 1988;35:721–725.
21. Steinmetz H, Fürst G, Freund HJ. Cerebral cortical localization: application and validation of the proportional grid system in MR imaging. *J Comput Assist Tomogr* 1989;13:10–19.
22. Levin DN, Pelizzari CA, Chen GTY, Chen CT, Cooper MD. Retrospective geometric correlation of MR, T, and PET images. *Radiology* 1988;169: 817–823.
23. Pelizzari CA, Chen GTY, Spelbring DR, Weichselbaum RR, Chen CT. Accurate three-dimensional registration of CT, PET, and/or MR images of the brain. J Comput Assist Tomogr 1989;13:20–26.
24. Dann R, Hoford J, Kovacic S, Reivich M, Bajcsy R. Evaluation of elastic matching system for anatomic (CT, MR) and functional (PET) cerebral images. *J Comput Assist Tomogr* 1989;13:603–611.
25. Pietrzyk U, Herholz K, Heiss WD. Three-dimensional alignment of functional and morphological tomograms. *J Comput Assist Tomogr* 1990;14: 51–59.
26. Herholz K, Pawlik G, Wienhard K, Heiss WD. Computer assisted mapping in quantitative analysis of cerebral positron emission tomograms. *J Comput Assist Tomogr* 1985;9:154–161.